

An insight into Capella (α Aurigae): from the extent of core overshoot to its evolutionary history

E. Marini¹, C. Ventura², M. Tailo³, P. Ventura¹, F. Dell’Aglì¹, M. Castellani¹

¹ INAF, Observatory of Rome, Via Frascati 33, 00077 Monte Porzio Catone (RM), Italy
email: ester.marini@inaf.it

² Dipartimento di Fisica, Sapienza Università di Roma, Piazzale Aldo Moro 5, I-00185 Roma, Italy

³ Dipartimento di Fisica e Astronomia Augusto Righi, Università degli Studi di Bologna, Via Gobetti 93/2, 40129 Bologna, Italy

2023

ABSTRACT

Context. The binary star α Aurigae (otherwise known as Capella) is extremely important to understand the core hydrogen and helium burning phases of the stars, as the primary star is likely evolving through the core helium burning phase, and the masses of the two components are $\sim 2.5 M_{\odot}$ and $\sim 2.6 M_{\odot}$, which fall into a mass range for which the extension of the core overshoot during the main sequence phase is uncertain.

Aims. We aim at deriving the extent of the core overshoot experienced during the core burning phases and testing the efficiency of the convective transport of energy in the external envelope, by comparing results from stellar evolution modelling with the results from the observations.

Methods. We consider evolutionary tracks calculated on purpose for the present work, for the primary and secondary star of Capella. We determine the extent of the extra-mixing from the core during the main sequence evolution and the age of the system, by requiring that the effective temperatures and surface gravities of the model stars reproduce those derived from the observations at the same epoch. We further check consistency between the observed and predicted surface chemistry of the stars.

Results. Consistency between results from stellar evolution modelling and the observations of Capella is found when extra-mixing from the core is assumed, the extent of the extra-mixed zone being of the order of $0.25 H_p$. The age of the system is estimated to be 710 Myr. These results allow to nicely reproduce the observed surface chemistry, particularly the recent determination of the $^{12}\text{C}/^{13}\text{C}$ ratio based on LBT (Large Binocular Telescope) and VATT (Vatican Advanced Technology Telescope) observations.

Key words. stars: evolution – stars: abundances – stars: interiors – binaries: general

1. Introduction

Understanding the physics of stars demands a thorough comprehension of how sources of different mass and metallicity evolve, and how the corresponding evolutionary tracks move across the Hertzsprung-Russell diagram. On this regards spectroscopic binaries prove a crucial tool, as they allow to infer the masses of the individual components with great precision, something that eases the comparison between the observational evidence and the theoretical predictions.

Among the various uncertainties still affecting the reliability of results from stellar evolution modelling, we stress those connected to the convective instability, namely: a) the extension of the convective core during the main sequence (MS) evolution of $M \geq 1.2 M_{\odot}$ stars; b) the extent of the mixing occurring during the red giant branch (RGB) ascending, which brings the surface regions of the stars in contact with internal zones, previously touched by nuclear activity; c) the efficiency of the convective transport of energy, which reflects into the overadiabaticity required in the outer layers of the envelope, thus the temperature gradient in those regions.

The size of the convective core determines the duration of the core hydrogen burning phase, the luminosity of the turn-off (the point in the HR diagram where the evolutionary tracks bend to the red after the consumption of the central hydrogen), and the luminosity of the “bump” defined by the evolutionary tracks

during the core helium burning phase. The discussions on this argument date back to the pioneering investigations aimed at calibrating the extent of overshooting from the convective core of stars evolving through the MS (Bressan et al. 1981; Renzini 1987; Chiosi et al. 1992). The debate was mainly focused on the need of assuming some overshoot from the convective core to reproduce the turn off morphology and luminosity of open clusters: among others, we recall the divergences regarding the cluster NGC 1866, with some research groups claiming that no-overshoot models were consistent with the observations (Brocato et al. 1989; Testa et al. 1999), while other teams stressed the need of assuming a significant extra-mixing from the core (Chiosi et al. 1989; Barmina et al. 2002). Further applications of core overshoot regarded the mass discrepancy problems of Cepheid stars (Bertelli et al. 1993). Recently, binary systems have been extensively used to determine the extent of core overshoot as a function of the stellar mass (Claret & Torres 2017, 2019; Morales et al. 2022). Further constrains on core overshoot were obtained by the determination of the initial-final mass relationship, based on the analysis of clusters turn-off and white dwarf cooling sequences (Cummings et al. 2019).

The inwards penetration of the bottom of the convective envelope during the RGB evolution is a natural consequence of the expansion and cooling of the external regions of the stars. This event, commonly known as first dredge-up (FDU), is easily predicted by stellar evolution modelling, and leads to the modi-

Table 1. Physical and chemical parameters of Capella

	Primary	Secondary	Ref.
Mass (M_{\odot})	2.5687 ± 0.0074	2.4828 ± 0.0067	Torres
T_{eff} (K)	4970 ± 50	5730 ± 60	Torres
$\log(g)$ (cgs)	2.691 ± 0.041	2.941 ± 0.032	Torres
T_{eff} (K)	4943 ± 23	5694 ± 73	Takeda
$\log(g)$ (cgs)	2.52 ± 0.08	2.88 ± 0.17	Takeda
$^{12}\text{C}/^{13}\text{C}$	17.8 ± 1.9	-	Sablowski
C/N	0.57 ± 0.06	3.30 ± 0.16	Torres
[Na/H]	-0.11 ± 0.10	$+0.09 \pm 0.08$	Torres
[Na/H]	$+0.414$	-0.216	Takeda

Notes. Torres: Torres et al. (2015), Takeda: Takeda et al. (2018), Sablowski: Sablowski et al. (2019).

fication of the surface chemistry of the star, which can be tested spectroscopically. On the other hand other processes might potentially alter the relative abundances of the various chemicals, in a modality which is still highly debated (Hedrosa et al. 2013; Pinsonneault 1997; Charbonnel & Lagarde 2010).

Capella (α Aurigae) is one of the most investigated and brightest binaries in the sky. Both components have estimated metallicity which is nearly solar (Fuhrmann 2011; Torres et al. 2015) and mass of the order of $2.5 M_{\odot}$ (Weber & Strassmeier 2011; Torres et al. 2015), a mass range extremely interesting for a number of reasons: a) this mass is just above the threshold value separating the sources experiencing the helium flash from those undergoing quiescent helium burning; b) the study of the extension of the core mass during the MS phase of the star with mass close to those of Capella’s components proves very important, since the investigations developed so far have shown that the trend of the extension of the extra-mixed region with mass exhibits a clear knee for masses below $\sim 2.5 M_{\odot}$ (Claret & Torres 2017); c) the studies focused on dust production by low and intermediate mass stars outlined that the stars of mass in the $2.5 - 3 M_{\odot}$ range are the most efficient dust manufacturers among the stellar sources, owing to the large carbon enhancement achieved during the asymptotic giant branch evolution, which triggers the production of large quantities of carbonaceous dust (Ventura et al. 2014; Dell’Agli et al. 2015, 2021).

The study of Capella proves therefore particularly important because of the tight estimate of the mass of both components and of their physical properties, mainly surface gravity and effective temperature (Torres et al. 2015; Takeda et al. 2018). Furthermore, the surface chemical composition was determined through atmosphere models and spectrum synthesis (Fuhrmann 2011; Torres et al. 2015; Takeda et al. 2018). The interpretation of these information allows to deduce the extension of the convective core during the MS evolution (which is crucial to reproduce the luminosity of both components) and of the extent of mixing from the base of the convective envelope during the FDU event (this is crucial to reproduce the observed chemical composition, particularly of the primary, which has presumably already experienced the FDU). The latter point has received renewed interest in the last few years, owing to the recent study by Sablowski et al. (2019), who used Large Binocular Telescope (LBT) and Vatican Advanced Technology Telescope (VATT), data to derive the surface carbon ratio of the primary star, obtaining a $^{12}\text{C}/^{13}\text{C} \sim 18-20$, significantly smaller than found in previous investigations (Tomkin et al. 1976). These observations were carried out with the Potsdam Echelle Polarimetric and Spectroscopic Instrument (PEPSI; Strassmeier et al. 2015) installed on

the pier of LBT. The ultra high-resolution mode provided by PEPSI ($R=250'000$) was used to derive the isotope ratio with the use of spectrum synthesis from the CN lines at 8004 \AA .

In the present study we reproduce the surface gravities and effective temperatures of the two components of Capella, and the surface chemical composition of the primary star (which are summarized in Table 1), by comparing with results from detailed stellar evolutionary models, calculated ad hoc for the two component of the system. The present analysis aims at the determination of the physical ingredients, particularly the extent of the core overshoot during the MS phase, which allow the best agreement with the observational evidence. The derivation of the age of the system will be the natural outcome of such an analysis. We will first consider the possibility that the primary and secondary stars evolved at constant mass, equal to those determined nowadays; we will also explore the case that the primary suffered mass loss while evolving during the RGB, and that formed with a higher mass than the current one.

The paper is structured as follows: the numerical and physical input used to calculate the evolutionary sequences used for the present analysis are described in section 2; a general description of the structural and evolutionary properties of the stars with mass similar to those of Capella’s components is given in section 3; in section 4 we reconstruct the evolutionary history of Capella, and discuss the extent of the core overshoot allowing the best agreement with the observational evidence; finally, the conclusions are given in section 5.

2. Stellar evolution modelling

The evolutionary sequences used in the present investigations were calculated by means of the ATON code for stellar evolution, in the version documented in Ventura et al. (1998), where the interested reader can find the details of the numerical structure of the code. The latest updates, including the nuclear network adopted and the micro-physics used, are described in Ventura & D’Antona (2009). Here we briefly discuss the physical and chemical ingredients of the code most relevant for the present study.

We considered model stars of initial mass in the $2.5 - 2.7 M_{\odot}$ range, with solar metallicity. The solar mixture was taken according to Lodders et al. (2009). The initial metallicity and helium mass fraction were set to $Z = 0.014$ and $Y = 0.268$, respectively.

2.1. The convective model

The location of the borders separating the regions of the stars characterized by convective motions from the radiatively stable layers are found via the classic Schwarzschild criterion. The temperature gradient with regions unstable to convective motions was calculated by means the full spectrum of turbulence (FST) model (Canuto & Mazzitelli 1991). The mixing length within the deep interiors of convective zones is assumed to be $\Lambda = z$, where z is the distance from the nearest convective border; close the boundaries we use $\Lambda = z + \beta H_p$; the free parameter was set to $\beta = 0.2$, in agreement with the calibration of the solar model given in Canuto & Mazzitelli (1991). Some further choices of β were considered for the present work.

2.2. Nuclear activity in convective regions

Nuclear burning and mixing of chemicals are coupled with the diffusive schematization described in Cloutman & Eoll (2019). The diffusive coefficient entering this treatment is $D = 1/3v_c\Lambda$, where the convective velocity v_c is calculated by means of Eqs. 88, 89, 90 of Canuto et al. (1996). For what attains mixing of chemicals beyond the formal borders, found via the Schwarzschild criterion, we consider an exponential decay of velocities, with a decay factor $\exp(\frac{1}{\zeta f_{\text{thick}}} \log \frac{P}{P_b})$. In the expression above P_b is the pressure at the formal boundary set by the Schwarzschild criterion, f_{thick} is the thickness of the convective region in fractions of the pressure scale height H_p , ζ is the parameter giving the e-folding distance of the convective velocity decay within radiatively stable regions, thus related to the extent of the extra-mixing occurring beyond the Schwarzschild border. The exponential approach to treat extra-mixing was applied also from the base of the convective envelope during the ascending of the RGB.

We note that convective velocities vanish at the formal border of convection. Therefore, as described in detail in section 2.2 of Ventura et al. (1998), the exponential decay is started by a point within the convective zone, where the pressure is 5% different with respect to the pressure at the convective boundary. As showed in Ventura et al. (1998), assuming that the decay starts from points where the pressure differences are 2%, 5% and 10% has no impact on the velocity profile.

The treatment adopted here is physically equivalent to those used in other investigations (Herwig et al. 1998; Torres et al. 2015) based on the exponential decay of velocities within radiative regions, as indicated by the numerical simulations by Freytag et al. (1996). On the other hand, the formalism is different, as in the present paper the decay is given as a function of pressure, whereas in the other papers the authors use the distance from the border: therefore the values of ζ that will be derived here cannot be compared directly with the results of the other investigations.

During the core He-burning phases we also considered diffusive extra-mixing, as described above. We did not assume any specific treatment of semi-convection (Castellani et al. 1971) in the present work, as the overshooting assumption pushes the boundary of the mixing zone beyond the critical point where the instabilities associated to semi-convection might arise (Caloi & Mazzitelli 1993).

3. The evolutionary properties of Capella's components

The primary and secondary components of Capella have masses around $2.5 M_\odot$. The current masses should not differ substantially from the initial values; this holds in particular for the secondary component, which is currently evolving through the initial part of the RGB phase, when no significant mass loss has occurred. Therefore, to understand the evolutionary properties of these stars, we focus on solar metallicity model stars of initial mass $2.5 M_\odot$.

These stars develop a convective core during the MS lifetime, thus the results obtained are sensitive to the assumed extra-mixing from the external border of the core during the hydrogen burning phase, which in the present work is described by the parameter ζ , introduced in section 2.2. The choice of ζ affects the extension of the mixed region beyond the formal border of the convective core during the MS, thus the duration of the H-burning phase and consequently the evolutionary time scale of the model stars.

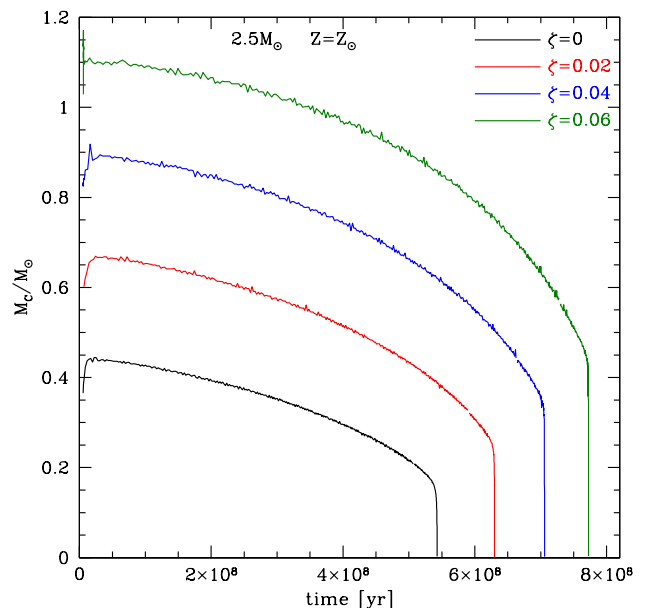


Fig. 1. Variation with the time of the mass of the central region of the star mixed by convective currents, of a model star of initial mass $2.5 M_\odot$ and solar metallicity during the hydrogen burning phase, adopting $\zeta=0$ (black line), $\zeta=0.02$ (red), $\zeta=0.04$ (blue) and $\zeta=0.06$ (green).

This can be seen in Fig. 1, where the different lines indicate the time variation of the mass of the region around the centre of the star where the surface chemistry shows trace of nuclear processing, which can be considered as the mass of the star within which convective mixing was sufficiently efficient to carry the products of the nuclear activity occurring in the deep interior. We find that the border of this region is located at the layer of the star where the diffusion coefficient, defined in section 2.2, drops below 10^{-10} c.g.s. unit: the masses reported in Fig. 1 refer to this layer. This choice implicitly implies that the definition of the masses shown in Fig. 1 is not physical. However, the quantities shown in the figure can be safely considered to deduce the extent of the regions of the stars touched by convective currents. Furthermore, the comparison of the individual tracks with the black one, which corresponds to the no-overshoot case, allows to infer the extent of the overshoot zone, according to the choice of ζ .

In all cases we recognize the typical behaviour of the convective cores during the MS, which shrinks as hydrogen is converted into helium, then vanish when the central hydrogen is exhausted. The largest extension (in mass) of this region is $\sim 0.45 M_\odot$ when no overshoot is assumed, and $\sim 1.1 M_\odot$ when $\zeta = 0.06$. Larger ζ 's also imply longer time scales, as higher quantities of hydrogen are transported within the innermost, nuclearly active regions. The duration τ_H of the H-burning phase changes from $\tau_H = 540$ Myr, for the no-overshoot case, to $\tau_H = 770$ Myr, for $\zeta = 0.06$. Roughly, we find that $\delta\zeta = 0.01$ corresponds to an age increase $\delta\tau_H \sim 40$ Myr.

The left panel of Fig. 2 shows the evolutionary tracks in the HR diagram of the $2.5 M_\odot$ model stars reported in Fig. 1. The

choice of ζ affects the morphology of the tracks in the region of the turn-off, for the reasons discussed earlier in this section, and the luminosity of the clump described by the tracks during the core helium burning phase. This is more clear in the right panel of Fig. 2, which is zoomed on the clump region. The thickest part of each track corresponds to the slowest part of the evolution, accounting for 90% of the overall post H-burning time. The luminosity range spanned by the clump is 40 – 50 L_{\odot} for the no-overshoot case, 45 – 65 L_{\odot} for $\zeta = 0.02$, 55 – 75 L_{\odot} for $\zeta = 0.04$, and 75 – 95 L_{\odot} for $\zeta = 0.06$.

The nuclear activity during the MS lifetime alters the chemical composition of the internal regions of the star, which is modified according to the proton capture nucleosynthesis experienced. The chemical stratification at the end of the MS turns extremely important to understand the change in the surface chemistry of the star taking place as a consequence of the FDU. Fig. 3 shows the mass fractions of various chemical species at the end of the core H-burning phase. The figure refers to the 2.5 M_{\odot} model star calculated with $\zeta = 0$ (black lines in Figg. 1 and 2).

The whole $M < 1.5 M_{\odot}$ region of the star is touched by the internal nucleosynthesis. We recognize the typical double step in the nitrogen profile, indicating the activation of the full CNO cycle for $M < 0.45 M_{\odot}$, and the plain CN cycle in the more external part of the core. This is confirmed by the depletion of the oxygen, which in the center of the star is depleted by a factor ~ 20 with respect to the initial quantity. Regarding the carbon isotopes, ^{12}C is depleted within the whole internal region of the star, whereas a peak in the ^{13}C profile is present at $M \sim 1.2 M_{\odot}$; both ^{12}C and ^{13}C are heavily depleted by more than a factor 100 in the innermost layers.

The chemistry of the region $M < 1 M_{\odot}$ is also affected by Ne-Na cycling, with the depletion of ^{22}Ne and the synthesis of sodium, whose central abundance exceeds the surface one by a factor ~ 4 .

4. Understanding the evolution of Capella

To reconstruct the past history of Capella we use evolutionary tracks calculated on purpose for the present investigation, for the primary and the secondary components, using the input described in section 2. The goal of this analysis is the determination of the combination of the parameters ζ and β , described in section 2.2 and 2.1, which allow to reach consistency between the results from modelling and those from the observations.

As a first step we require that the evolutionary tracks of the model stars in the effective temperature - gravity plane reproduce the results obtained from the observations. We will consider first the study by Torres et al. (2015), then the more recent work by Takeda et al. (2018): the corresponding observational boxes for the two components of the system are shown in grey and yellow, respectively, in Fig. 4. The fit of the surface gravities will lead to select the appropriate range of values of ζ . β affects mainly the effective temperature, thus possible changes with respect to the value required to reproduce the evolution of the Sun will be considered only in the case that the effective temperatures of the stars are not reproduced by modelling.

The second step of this analysis will be to further restrict the range of parameters to be considered, by requiring that the model stars of the primary and secondary evolve through the observational boxes shown in Fig. 4 at the same time. This will also allow the determination of the age of the system.

The final step of this procedure will be to check consistency between the expected change of the surface chemistry, driven by

the FDU, and the measured surface abundances of the various chemical species.

4.1. The determination of core extra-mixing

Based on the high highly precise (~ 0.3) masses obtained by Torres et al. (2015) and reported in Table 1, we first start by considering model stars of mass 2.6 M_{\odot} and 2.5 M_{\odot} for the primary and secondary star, respectively; this choice implicitly assumes that negligible mass loss occurred during the previous evolutionary phases. We will also consider the possibility that the primary star was initially more massive than nowadays, thus invoking some mass loss during the RGB ascending.

Fig. 4 shows the evolutionary tracks of model stars of mass 2.5 M_{\odot} and 2.6 M_{\odot} , calculated with different ζ 's. The observational boxes for both components of Capella, as found by Torres et al. (2015), are shown as grey rectangles. From the results shown in Fig. 4 we deduce that only ζ 's in the 0.03-0.04 range can be considered: values of ζ external to this range do not allow to fit the surface gravity (hence the luminosity) of both stars.

As discussed previously, we also require that the two stars evolve through the respective observational box at the same epoch. In Fig. 5 we show the evolution of the surface gravity of different model stars, calculated with different values of ζ . The surface gravities derived by Torres et al. (2015) are shown as coloured regions. We see in Fig. 5 that consistency is found in the $\zeta = 0.04$ case, which leads to an estimated age of 710 Myr. This is more evident in the right panel of Fig. 5, which is focused on the region inside the black box. We note that this choice corresponds to an assumed instantaneous extra-mixing from the core of $\sim 0.25 H_p$.

On the other hand, adopting $\zeta = 0.03$ does not allow the simultaneous fit of both components: indeed in this case the age derived on the basis of the modelling of the secondary star, i.e. 670 Myr, is at odds with the age derived for the primary, as the latter star is expected to reach the observed gravities only during the final part of the clump evolution, at an age of 710 Myr.

For what concerns the choice of the parameter β entering the expression of the mixing length in the FST modelling, the results reported in Fig. 4 suggest that adopting $\beta = 0.2$ allows to reproduce the effective temperatures derived for both the components of Capella, although a slightly higher value cannot be ruled out on the basis of the present analysis. This is the first confirmation, to date, that the same quantity originally derived by Canuto & Mazzitelli (1991) to reproduce the evolution of the Sun can be applied in a different physical situation, such as the convective envelope of a star evolving through the RGB and the core helium burning phase.

According to the present analysis Capella is ~ 80 Myr younger than found by Torres et al. (2015), based on the PARSEC isochrones of Bressan et al. (2012). The reason for this difference is mainly due to the different chemistry adopted: Torres et al. (2015) use a slightly sub-solar metallicity and initial helium $Y = 0.272$, whereas we use solar metallicity and helium $Y = 0.268$. Both the higher metallicity and the lower helium adopted here favour older ages, of the order of ~ 40 Myr. Further differences with respect to the PARSEC models, which explain the residual age difference between us and Torres et al. (2015), are the solar mixture adopted (we use the mixture by Lodders et al. (2009), whereas Bressan et al. (2012) assume the element distribution by Grevesse & Sauval (1998)), and the prescription for core overshoot.

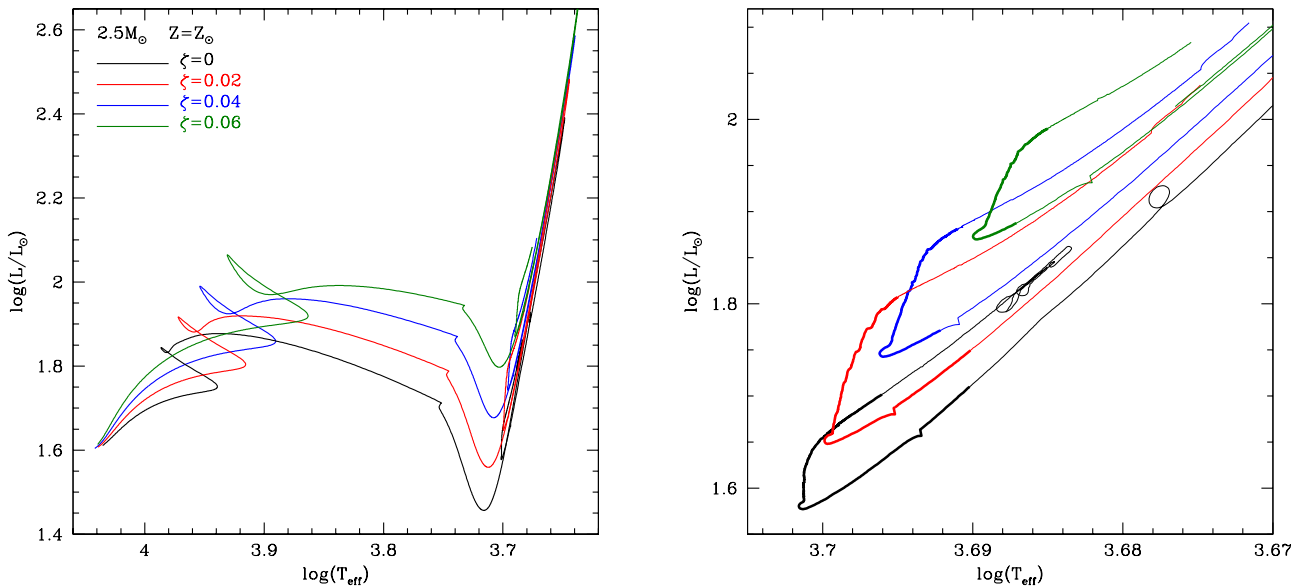


Fig. 2. Left: Evolutionary track of $2.5M_{\odot}$ model star with solar metallicity on the HR diagram, calculated with the same values of ζ as Fig. 1. Right: Same as left panel, but focusing on the clump region, where the slowest part of the evolution is highlighted by a thick line.

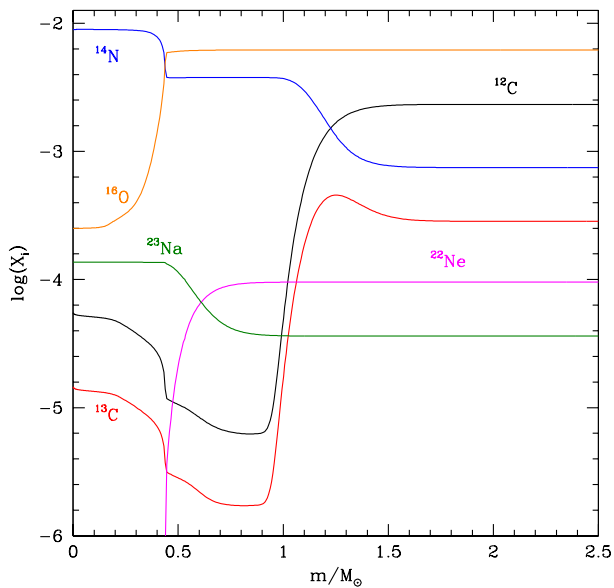


Fig. 3. Internal chemical stratification of a model star of $2.5M_{\odot}$ with solar metallicity at the end of the core hydrogen burning phase, calculated by assuming no overshoot ($\zeta=0$).

4.2. A test of mass-loss during the RGB

We also considered the possibility that the primary star experienced mass loss during the previous evolutionary phases, so that it descends from a higher mass progenitor. On the numeri-

cal side, when a plain mass loss description such as Reimers' is adopted, the decrease in the total mass by the time that the star reaches the core He-burning phase is within $0.01 M_{\odot}$, for any reasonable choice of the free parameter entering the Reimers' recipe. However, we decided to investigate the effects of some mass loss, even significantly higher than found via the Reimers' description.

we first tested the case that the initial mass was $2.7 M_{\odot}$. In this case we find consistency with the temperature and gravity derived from the observations of the primary, by assuming $\zeta = 0.035$. However, this choice would pose severe issues on the side of the evolutionary times, as the secondary star would attain the corresponding observational quantities ~ 50 Myr ahead of the primary. To maintain simultaneity we should claim that the overshoot from the core of the secondary star was smaller, of the order of $\zeta = 0.02$; however, as discussed earlier in this section (see also Fig. 4), this choice is ruled out, as it does not allow to fit the surface gravity of the secondary component, given in Torres et al. (2015).

4.3. The study by Takeda et al. (2018)

In a recent paper Takeda et al. (2018) published a new study on Capella, where the elemental abundances were estimated by the disentangled spectrum of the two components. The effective temperatures found by Takeda et al. (2018) are in substantial agreement with those given in Torres et al. (2015), with the only difference that the error associated to the determination of the temperature of the primary, 23 K, is significantly lower than the errors reported in the study by Torres et al. (2015). The comparison between the surface gravities derived in the two studies outlines that the gravities derived in Takeda et al. (2018) are significantly lower than those given by Torres et al. (2015). While in the case of the secondary star consistency is found when the error bars are taken into account, in the case of the primary there is

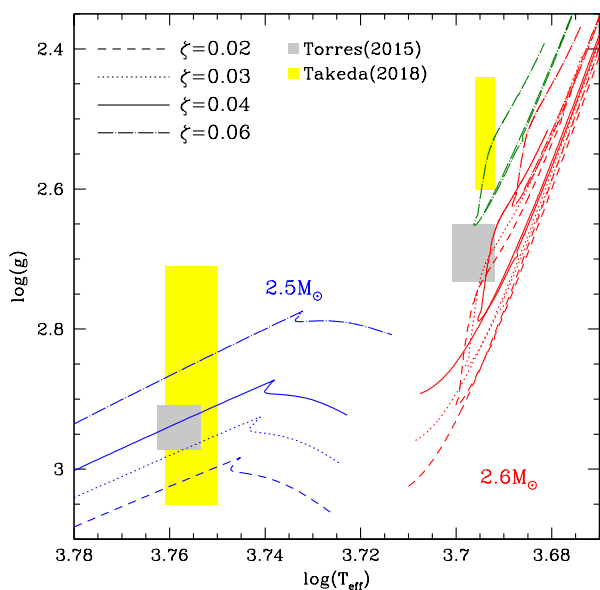


Fig. 4. Evolutionary tracks on the $\log(T_{\text{eff}}) - \log(g)$ plane of model stars of mass $2.5 M_{\odot}$ (blue lines) and $2.6 M_{\odot}$ (red), calculated by assuming different values of the overshoot parameter ζ . The green line refers to a $2.6 M_{\odot}$ model star obtained by assuming $\zeta = 0.06$ and an FST parameter $\beta = 0.27$. Grey and yellow rectangles indicate the error boxes for the two components of Capella given, respectively, in Torres et al. (2015) and Takeda et al. (2018).

a difference $\delta(\log g) = 0.17$ between the two studies, which can be reduced at most to $\delta(\log g) = 0.05$ when the corresponding error bars are considered.

To reproduce the surface gravities given by Takeda et al. (2018) we calculated new evolutionary sequences for both the components of Capella, with values of ζ higher than those previously discussed: this is because the lower gravities of the primary imply higher luminosities. We note that given the large error associated to the derivation of the surface gravity of the secondary star, this part of the study was essentially focused on the fit of the observed parameters of the primary.

Consistency with the surface gravity of the primary star is found when a $2.6 M_{\odot}$ is evolved with $\zeta = 0.06$, which corresponds to an instantaneous overshoot from the outer border of the convective core during the H-burning phase of $0.36 H_{\text{p}}$. As shown in Fig. 4, in this case the effective temperature during the helium burning phase, is slightly cooler with respect to the values given in Takeda et al. (2018), which required to use a higher FST parameter: the choice $\beta = 0.27$ allows a nice fit of the results from the observations (green track in Fig. 4).

4.4. Which will be the final mass of the primary component of Capella?

The main difference between the conclusions drawn when using the gravities given in Torres et al. (2015) and those by Takeda et al. (2018) is the extension of the extra-mixed zone during the MS evolution: in the former case we find $\zeta = 0.04$, which corresponds to a $0.25 H_{\text{p}}$ size, whereas in the latter case we derive $\zeta = 0.06$, which corresponds to $0.37 H_{\text{p}}$.

To test the possibility of discriminating on the basis of the initial-final mass relationship derived by Cummings et al. (2019), we extended the computations of model stars of mass $2.6 M_{\odot}$ until the first thermal pulse, thus at the beginning of the asymptotic giant branch (AGB) phase. The purpose of this test was to check whether either of the two values given above leads to inconsistency with the Cummings et al. (2019) law.

In the $\zeta = 0.04$ case we find a core mass of $0.53 M_{\odot}$, whereas when $\zeta = 0.06$ is adopted we find $0.57 M_{\odot}$. Unfortunately this difference prevents any possibility of discriminating between the two scenarios. As shown in Ventura et al. (1998), model stars that attain core masses at the beginning of the AGB evolution similar to those mentioned above end up the AGB phase with a final mass of $\sim 0.7 M_{\odot}$, which is anyway consistent with the expectations based on the study by Cummings et al. (2019).

4.5. The surface chemical composition

In Fig. 6 we describe the evolution of the primary star during the evolutionary phases close to the occurrence of the FDU. The figure refers to the $2.6 M_{\odot}$ model star calculated with $\zeta = 0.04$, discussed earlier in this section. The quantities shown are the mass of the region of the star below the bottom of the convective envelope, the surface sodium and the $^{12}\text{C}/^{13}\text{C}$ and C/N ratios.

During the FDU the convective envelope penetrates inwards and grows in mass, up to including $\sim 2 M_{\odot}$ of the star. The base of the convective mantle reaches regions of the star whose chemical composition was altered by nuclear activity; the typical stratification of the star at the end of the core hydrogen burning phase, before the occurrence of the FDU, is shown in Fig. 3. The occurrence of FDU favours the increase in the surface nitrogen and sodium, the decrease in the surface carbon, with an overall increase in $^{12}\text{C}/^{13}\text{C}$.

The latter quantity proved a severe issue in the attempt of reconstructing the previous history of Capella, because the value given by Tomkin et al. (1976), $^{12}\text{C}/^{13}\text{C} \sim 27$, was significantly higher than that found from stellar evolution modelling. The agreement between the theoretical expectations and the observational results is now possible thanks to the recent work by Sablowski et al. (2019). The authors, based on LBT and VATT observations carried out with PEPSI, found that the surface $^{12}\text{C}/^{13}\text{C}$ of the primary star is 17.8 ± 1.9 , significantly lower than that found by Tomkin et al. (1976). The reason for this difference is likely the fact that Tomkin et al. (1976) used an incorrect light ratio between the two components, thus underestimating the equivalent width measurements of the CN lines by 6 – 11% (Torres et al. 2009); on the other hand, the analysis by Sablowski et al. (2019) benefited from the remarkable performances of PEPSI, which made it possible to obtain ultra-high resolution spectra with high signal-to-noise ratio (~ 2000), thus allowing an estimation of $^{12}\text{C}/^{13}\text{C}$ of the primary star of Capella with unprecedented reliability. As shown in Fig. 6, the new measurement is in nice agreement with results from stellar evolution modelling. This result indicates that the surface chemistry of the primary star was altered by the effects of the FDU only, with no additional contribution from some other mechanisms, often invoked to occur during the RGB phase, to explain, e.g., the low $^{12}\text{C}/^{13}\text{C}$ detected in open cluster stars (Gilroy & Brown 1991). This is consistent with the predictions by Charbonnel & Lagarde (2010), who find that neither thermohaline nor rotational mixing alter substantially the surface chemistry of stars in the mass domain explored here, during the RGB phase.

Concerning the C/N ratio, as shown in Fig. 6, we find that the expected value (~ 0.65) is slightly in excess of the value reported

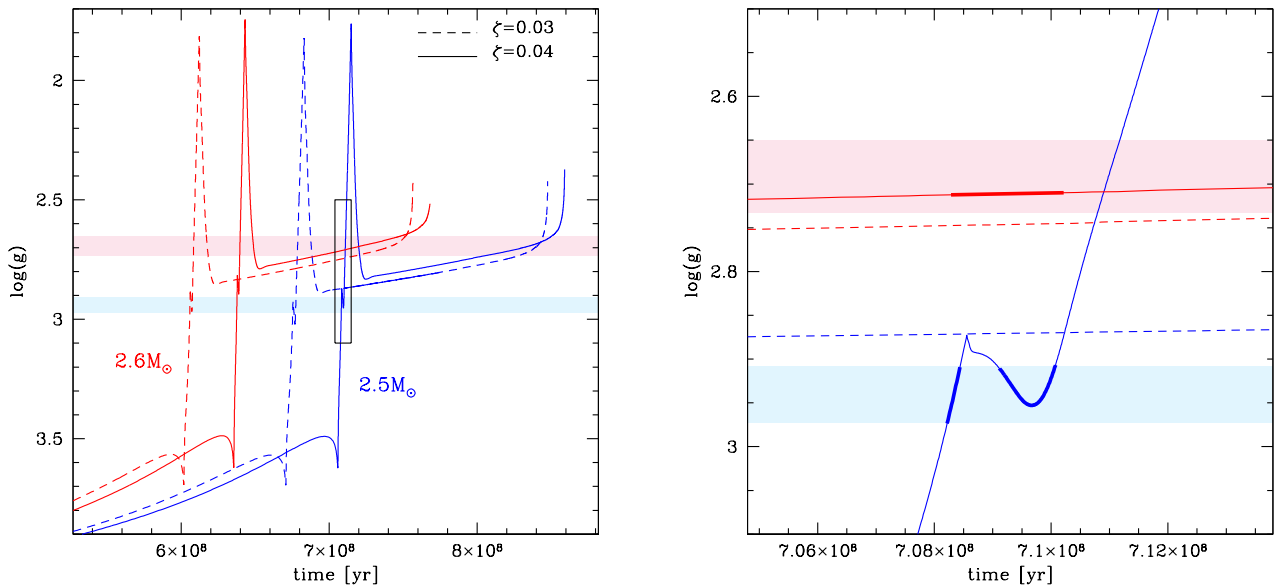


Fig. 5. Time variation of the $\log(g)$ of model stars of mass $2.5 M_{\odot}$ (blue lines) and $2.6 M_{\odot}$ (red), calculated by assuming $\zeta = 0.03$ and $\zeta = 0.04$. Coloured regions indicate the error associated to the derivation of the surface gravity for the two components of Capella (pink - primary, cyan - secondary) given in Torres et al. (2015). The black box on the left panel is zoomed on the right, in which the thick lines highlight the simultaneous fit of both components.

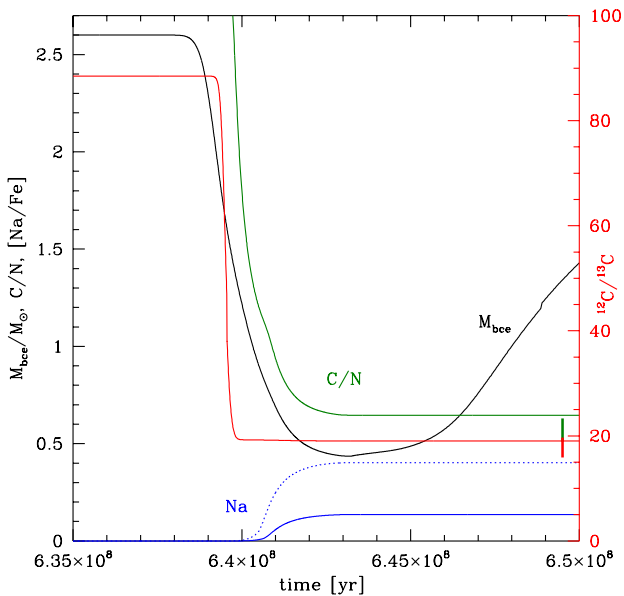


Fig. 6. Time variation of the mass at the bottom of the convective envelope (black, scale on the left), of the surface sodium (blue, scale on the left), and of the carbon isotopic ratio (red, scale on the right) of a $2.6 M_{\odot}$ model star, calculated with an overshoot parameter $\zeta = 0.04$. The plot is focused on the epoch during which the FDU takes place. The dashed, blue line indicates the variation of the surface sodium abundances of a model star calculated by assuming that the initial neon is enhanced by a factor 3.

in Torres et al. (2015), $C/N \sim 0.57$: this might be a consequence of the fact that the lines used to estimate the C and N abundances do not fully represent the abundances in the photosphere (see discussion in Torres et al. 2015, on this argument).

Regarding the surface sodium of the primary, the results from Torres et al. (2015) and Takeda et al. (2018) differ significantly: while according to Torres et al. (2015) the star shows no sign of Na enrichment, Takeda et al. (2018) find that the primary is sodium enriched by 0.4 dex. The latter result can be hardly explained within the context of the FDU, as the expected increase in the surface sodium is $\delta[Na/Fe] \sim 0.2$ (see Fig. 6). The assumption of extra-mixing is of little help here, as the consequent increase in the final $[Na/Fe]$ is within 0.05 dex. Among the various possibilities, we take into account that the neon is underestimated, such that the initial neon is higher than that proposed by Lodders et al. (2009). We explored various possibilities, and found that a sodium enrichment in agreement with the results from Takeda et al. (2018) is obtained by assuming an initial neon a factor 3 higher than in Lodders et al. (2009). A discussion regarding the initial neon of solar metallicity stars is definitively beyond the scopes of the present investigation; however, we point out that the neon enhancement invoked here, of the order of +0.5 dex, is consistent with the conclusions reached by Bahcall et al. (2005), where a higher neon is required to reconcile the predictions from solar modelling with heliosismological measurements. We leave this problem open.

The results shown in Fig. 6 were obtained by assuming extra-mixing from the convective core during the H-burning and from the bottom of the envelope during the RGB phase. The latter assumption has no effect on the evolutionary time scale and on the excursion of the evolutionary track across the HR diagram, but might potentially alter the extent of the inwards penetration of the envelope, thus the change in the surface chemical composi-

tion following the occurrence of the FDU. To this aim we calculated further evolutionary sequences, where we explored different values of the ζ parameter in the 0–0.06 range to describe the overshoot from the base of the surface convection; for the core we used $\zeta = 0.04$ in all cases.

In the no-overshoot case we find differences in the final abundances of ^{12}C , ^{13}C and ^{14}N of the order of 10%, while the final sodium is 15% lower than for the $\zeta = 0.04$ case. In this case the $^{12}\text{C}/^{13}\text{C}$ and C/N ratio are significantly higher than those resulting from the spectroscopic analysis, whereas the discrepancy in the surface sodium between theory and the observations is amplified. On the other hand, when ζ is chosen in the 0.02–0.06 range, the results turn out almost independent of ζ . The reason for this is that for any choice of $\zeta \geq 0.02$ the base of the mixed regions approaches the H-burning shell, thus convection is pushed outwards.

This exploration shows that some extra-mixing from the base of the convective zone is required to reproduce the observations, although it is not possible to assess the extension of the extra-mixed zone in detail.

5. Conclusions

The evolutionary history of stars forming the binary system α Aurigae, or Capella, is reconstructed, by means of the comparison between results from stellar evolution modelling and those derived from observations. The conclusions reached in this work have been mostly based on the analysis of the primary star, which is likely evolving through the core helium burning phase, and has already experienced the change in the surface chemical composition favoured by the occurrence of the first dredge-up; conversely, the secondary star is currently evolving through the early phase of the red giant branch, thus the derived luminosity and chemical composition turn out of little help in this context.

The results from the present analysis indicate that Capella formed ≈ 710 Myr ago. The comparison between the derived surface gravity and effective temperature of the primary star confirm that extra-mixing from the convective core occurred during the main sequence phase, with the extension of the extra-mixed zone being of the order of 0.25 H_p . This result is in agreement with previous works focused on the determination of the size of the convective cores of stars of mass similar to those of Capella's components. Regarding the full spectrum of turbulence convection modelling used here, we find that the expression for the mixing length required to reproduce the evolution of the Sun is consistent with the effective temperatures found for the primary and secondary stars of Capella.

The estimate of the core overshoot must be reconsidered upwards if we consider a more recent, lower estimate of the surface gravity (hence a higher luminosity) of the primary component, which leads to a larger size of the overshoot zone, of the order of 0.37 H_p .

The nowadays observed surface chemistry of the primary star can be explained as a result of the occurrence of the first dredge-up only: we confirm previous results from detailed stellar evolution modelling, that stars of mass $\sim 2.5 M_\odot$ during the RGB phase experience no additional mixing mechanisms, such as thermohaline and rotational mixing, likely taking place in the lower mass counterparts. This conclusions relies on the observed C/N and $^{12}\text{C}/^{13}\text{C}$ ratios, the latter having been recently found using high-resolution spectra obtained with PEPSI at LBT and VATT. Recent results from detailed model-atmosphere analysis of the disentangled spectrum outline a significant sodium en-

hancement, of the order of 0.4 dex, which we tentatively explain by invoking a higher neon content of the star.

Acknowledgements. EM is indebted to Guillermo Torres and Yoichi Takeda for the helpful discussions. EM acknowledges support from the INAF research project "LBT - Supporto Arizona Italia". MT acknowledges support from the ERC Consolidator Grant funding scheme (project ASTEROCHRONOMETRY, <https://www.asterochronometry.eu>, G.A. No. 772293).

References

- Bahcall, J. N., Basu, S., & Serenelli, A. M. 2005, *ApJ*, 631, 1281
 Barmina, R., Girardi, L., & Chiosi, C. 2002, *A&A*, 385, 847.
 Bertelli, G., Bressan, A., Chiosi, C., et al. 1993, *ApJ*, 412, 160
 Bressan, A., Bertelli, G., Chiosi, C. 1981, *A&A*, 102, 25.
 Bressan, A., Marigo, P., Girardi, L., et al. 2012, *MNRAS*, 427, 127
 Brocato, E., Buonanno, R., Castellani, V., et al. 1989, *ApJS*, 71, 25
 Caloi, V. & Mazzitelli, I. 1993, *A&A*, 271, 139
 Canuto, V. M. & Mazzitelli, I. 1991, *ApJ*, 370, 295
 Canuto, V. M., Goldman I., Mazzitelli, I. 1996, *ApJ*, 473, 550
 Castellani, V., Giannone, P., & Renzini, A. 1971, *Ap&SS*, 10, 355
 Charbonnel, C., Lagarde, N., 2010, *A&A*, 522, A19.
 Chiosi, C., Bertelli, G., Meylan, G., et al. 1989, *A&A*, 219, 167
 Chiosi, C., Bertelli, G., Bressan, A., 1992, *AR&A*, 30, 235.
 Claret, A., Torres, G., 2017, *ApJ*, 849, 18.
 Claret, A., Torres, G., 2019, *ApJ*, 876, 134.
 Cloutman, L. D., Eoll, J. G., 1976, *ApJ*, 206, 548.
 Charbonnel, C. & Lagarde, N. 2010, *A&A*, 522, A10
 Cummings, J. D., Kalirai, J. S., Choi, J., et al. 2019, *ApJ*, 871, L18.
 Dell'Agli, F., Ventura, P., Schneider, R., et al. 2015, *MNRAS*, 447, 2992
 Dell'Agli, F., Marini, E., D'Antona, F., et al. 2021, *MNRAS*, 502, L35
 Freytag, B., Ludwig, H.-G., & Steffen, M. 1996, *A&A*, 313, 497
 Fuhrmann K., 2011, *ApJ*, 742, 42
 Gilroy, K. K. & Brown, J. A. 1991, *ApJ*, 371, 578
 Grevesse, N. & Sauval, A. J. 1998, *Space Sci. Rev.*, 85, 161
 Hedrosa, R. P., Abia, C., Busso, M., et al. 2013, *ApJ*, 768, L11.
 Herwig, F., Schoenberner, D., & Bloeker, T. 1998, *A&A*, 340, L43
 Lodders, K., Palme, H., & Gail, H.-P. 2009, *Landolt BÖrstein*, 4B, 712
 Morales, L. M., Sandquist, E. L., Schaefer, G. H., et al. 2022, *AJ*, 164, 34.
 Pinsonneault, M. 1997, *ARA&A*, 35, 557
 Renzini, A. 1987, *A&A*, 188, 49
 Sablowski, D. P., Järvinen, S., Ilyin, I., Strassmeier, K. G., 2019, *A&A*, 622, L11.
 Strassmeier K. G., Reegen P., Granzer T., 2001, *AN*, 322, 115.
 Strassmeier K. G., Ilyin I., Järvinen A., Weber M., Woche M., Barnes S. I., Bauer S.-M., et al., 2015, *AN*, 336, 324
 Takeda, Y., Hashimoto, O., Honda, S., 2018, *ApJ*, 862, 57.
 Testa, V., Ferraro, F. R., Chieffi, A., et al. 1999, *AJ*, 118, 2839
 Tomkin J., Luck R. E., Lambert D. L., 1976, *ApJ*, 210, 694.
 Torres, G., Claret, A., Young, P. A., 2009, *ApJ*, 700, 1349.
 Torres, G., Claret, A., Pavlovski, K., Dotter, A., 2015, *ApJ*, 807, 26.
 Ventura, P., Zeppieri, A., Mazzitelli, I., et al. 1998, *A&A*, 334, 953
 Ventura, P. & D'Antona, F. 2009, *A&A*, 499, 835
 Ventura, P., Dell'Agli, F., Schneider, R., et al. 2014, *MNRAS*, 439, 977
 Ventura, P., Karakas, A., Dell'Agli, F., et al. 2018, *MNRAS*, 475, 2282
 Weber, M., Strassmeier, K. G., 2011, *A&A*, 531, A89